Available online at www.sciencedirect.com
SCIENCE DIRECT
Journal of Magnetic Resonance 181 (2006) 154–161
JMR Journal of Magnetic Resonance
www.elsevier.com/locate/jmr

Effect of nitrogen dioxide on the EPR property of lithium octa-*n*-butoxy 2,3-naphthalocyanine (LiNc-BuO) microcrystals

Ramasamy P. Pandian [a], Vinh Dang [a], Periakaruppan T. Manoharan [b], Jay L. Zweier [a], Periannan Kuppusamy [a,*]

[a] *Center for Biomedical EPR Spectroscopy and Imaging, Department of Internal Medicine, Davis Heart and Lung Research Institute, The Ohio State University, Columbus, OH 43210, USA*
[b] *Department of Chemistry/SAIF, Indian Institute of Technology/Madras, Chennai, India*

Received 10 February 2006; revised 5 April 2006
Available online 11 May 2006

Abstract

Lithium octa-*n*-butoxy-naphthalocyanine (LiNc-BuO) is a stable free radical that can be detected by electron paramagnetic resonance (EPR) spectroscopy. Previously we have reported that microcrystals of LiNc-BuO exhibit a single sharp EPR peak, whose width varies linearly with the partial pressure of paramagnetic molecules such as oxygen and nitric oxide. In this report, we present the effect of nitrogen dioxide (NO_2), which is also a paramagnetic molecule, on the EPR properties of LiNc-BuO. The gas-sensing property of LiNc-BuO is attributed to the open molecular framework of the crystal structure which is arranged with wide channels capable of accommodating large molecules such as NO_2. The EPR linewidth of LiNc-BuO was highly sensitive to the partial pressure of NO_2 in the gas mixture. The line-broadening was quick and reversible in the short-term for low concentration of NO_2. However, the EPR signal intensity decreased with time of exposure, apparently due to a reaction of NO_2 with LiNc-BuO crystals to give diamagnetic products. The results suggested that LiNc-BuO may be a useful probe for the determination of trace amounts of NO_2 using EPR spectroscopy.

Keywords: Electron paramagnetic resonance (EPR); Phthalocyanine; Naphthalocyanine; Oxygen; Nitric oxide; Nitrogen dioxide

1. Introduction

The gaseous oxides of nitrogen and sulfur that are produced during the combustion and subsequent emission into the environment of petroleum products are of concern to the health of living organisms. The search for suitable materials or devices that can be used as reliable sensors of these harmful gases has attracted the attention of many researchers in recent years [1–3]. Most conventional gas sensors are made of metal oxides [4]. The inadequacy of these sensors is that they require very high working temperatures, usually 300–400 °C. To optimize the operating conditions of these sensors, thin-film sensors have been developed [5–7]. These films still require temperatures above 100 °C. Recently, there has been considerable interest in exploiting organic materials such as porphyrin [8], phthalocyanine [9–11], and doped conductive polymers [12] for gas-sensing applications. Hanawa et al. [13] have shown that electropolymerized polypyrrole films exhibit noticeable room temperature gas sensitivities to electron acceptor gases such as phosphorous trichloride, sulphur dioxide, and nitrogen dioxide (NO_2). They also have investigated the gas-sensing properties of polythiophene films and found an irreversible change in conductivity after exposure to gases [14].

Phthalocyanines, one of the most suitable of all organic functional materials, have found wide applications in areas of non-linear optics (including optical limitation), Xerography (as photoconductors), optical data storage (as the laser absorption layer within recordable compact discs), molecular electronics, photodynamic cancer therapy, solar energy

* Corresponding author. Fax: +1 614 292 8454.
E-mail address: kuppusamy.1@osu.edu (P. Kuppusamy).

1090-7807/$ - see front matter © 2006 Elsevier Inc. All rights reserved.
doi:10.1016/j.jmr.2006.04.004

conversion, catalysis, and also as the active constituents of gas sensors [15,16]. The effect of NO_2 on the conducting properties of sublimed phthalocyanine films has been reported [17]. The gas specificity of the phthalocyanine structure may be developed by appropriately placing metals in the cavity or creating organic substituents at the periphery [17]. It has been established that the electrical properties of the phthalocyanines are modulated upon exposure to gases such as NO_2 or ammonia [17]. This opens a promising route in developing gas detectors using phthalocyanine derivatives as a chemically sensitive component [17]. The gas adsorption/desorption processes of metallophthalocyanines (MPc) depend not only on the material's redox potentials but also on their surface morphology and molecular arrangement, since the latter properties are expected to affect both the charge-transfer interaction and charge-carrier transport [18]. Among the metal-incorporated phthalocyanines, lead phthalocyanine is the most interesting and intensively studied material [19–23]. This material has been reported to be better than other phthalocyanines for the detection of oxidizing gases.

We recognize that gas-sensing features, such as accuracy, response time, reproducibility, and reversibility can be enhanced by certain physical or chemical phenomena that occur at the gas-material interface. A better understanding of such changes occurring in MPc upon gas exposure may contribute to improvement in sensor function. Naphthalocyanine (which has a larger π-conjugated system than phthalocyanine) and its derivatives have been widely studied in recent years as new types of functional materials because of their special optical and electrical properties, biological activity, good processability, structural variety, and functional adjustment [24–28]. It is especially important to realize that this kind of materials exhibits much better sensitivity to gases tested at room temperature, with potential applications [9,10,15,29]. In continuation of our reports [30–32] on lithium phthalocyanine (LiPc) and lithium naphthalocyanine (LiNc) as sensors for O_2 and NO, we have extended our investigation to the NO_2 gas-sensing properties of the naphthalocyanines using EPR spectroscopy. We have recently reported a new probe, namely, lithium octa-*n*-butoxy-2,3-naphthalocyanine (LiNc-BuO, Fig. 1), having favorable crystalline packing and paramagnetic behavior for in vivo biological oximetry [33]. In this paper, we report our findings on the effect of the NO_2 gaseous molecule on the paramagnetic properties of LiNc-BuO, measured using EPR spectroscopy, at room temperature. The results demonstrate that the EPR lineshape of LiNc-BuO is highly sensitive to NO_2. The effect is reversible for short periods of exposure to low concentrations of NO_2 while at higher concentrations, or on prolonged exposure, an irreversible loss of paramagnetism is observed.

2. Materials and methods

Microcrystals of lithium 5,9,14,18,23,27,32,36-octa-*n*-butoxy-2,3-naphthalocyanine (LiNc-BuO) were prepared as reported [33]. Fig. 1 shows the molecular structure and crystalline packing of LiNc-BuO [34]. 1% NO_2 (+99% N_2) was purchased from Praxair (Danbury, CT, USA). 100% NO_2 gas was prepared by the reaction of concentrated nitric acid on metallic copper turnings as reported [35]. It should be noted that NO_2 would exist in equilibrium with dinitrogen tetroxide, N_2O_4, which is diamagnetic. The N_2O_4 would exist in the liquid phase with a purple color and the NO_2 would exist in the gas phase with a reddish brown color. In the case of 1% NO_2 (+99% N_2) mixture, the NO_2 would be pulled from the vapor headspace of the NO_2 cylinder. This would make the 1% NO_2 essentially all NO_2 with very little N_2O_4. However, the presence of significant levels of the dimer cannot be ruled out in our 100% NO_2 preparation. Since the LiNc-BuO preparations showed some small variations in the anoxic linewidth from batch to batch, this study used particles obtained from a single preparation.

A small amount of LiNc-BuO crystals (~10 μg) was encapsulated in a 0.8-mm diameter gas-permeable Teflon

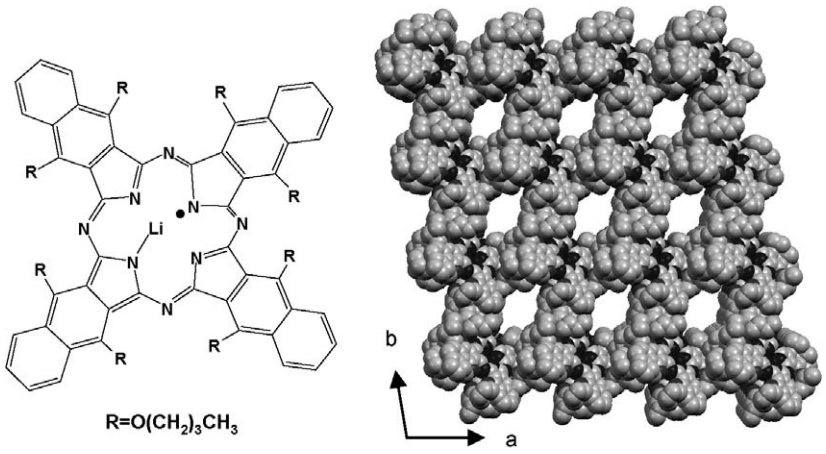

Fig. 1. Molecular structure of lithium 5,9,14,18,23,27,32,36-octa-*n*-butoxy-2,3-naphthalocyanine (LiNc-BuO) neutral radical and a perspective view of its crystalline packing (space-filling model) as viewed along the *c*-axis [34]. The structure shows wide open channels with cross-sectional dimensions 10×6 Å^2.

tube (Zeus Industrial Products, Orangeburg, SC, USA). The tube was sealed at both ends and inserted into a 3-mm quartz EPR tube. NO_2 was flushed into the EPR tube using gas-impermeable silicon tubing. The EPR tube was placed inside a TM_{110} microwave cavity (X-band) ensuring that the sample was at the center of the active volume of the resonator. The flow rate of the gas was maintained at 2000 ml/min. The total pressure inside the EPR tube was 760 mmHg, since the other end of the EPR tube was open to the atmosphere.

EPR measurements were carried out at 9.78 GHz (X-band) using a Bruker model ER300 EPR spectrometer (Billerica, MA, USA). Data acquisition and analysis were performed using a personal computer (PC) interfaced to the spectrometer. Unless mentioned otherwise, the EPR linewidths reported in this manuscript are the peak-to-peak width (ΔB_{pp}) of the first derivative spectra. The EPR spectral intensity was obtained by double-integration of the first derivative spectra. The results were expressed as mean ± SD (standard deviation) obtained from at least three independent experiments.

Infra-red (IR) spectra were recorded using a Perkin-Elmer SpectrumOne FT-IR spectrophotometer (Wellesley, MA, USA).

3. Results and discussion

First, it should be noted that diatomic gases like O_2, N_2, and NO can easily enter the channels located in the crystals of LiNc-BuO and are expected to be freely mobile within these channels [33,34]. Also, O_2 and NO, due to the unpaired spins (paramagnetism) in these molecules, are noted for their broadening effect on the EPR spectrum of LiNc-BuO [33,34]. In the absence of the paramagnetic gases, LiNc-BuO showed a very narrow EPR line ($\Delta B_{pp} = 0.280 \pm 0.005$ G) as a result of fast exchange of lattice (host) spins via the so-called exchange narrowing effect [36]. However, entering of the paramagnetic (guest) molecules into the host lattice can break this exchange by interacting with the host spins, both by Heisenberg exchange and/or dipolar interaction causing an increase in the observed linewidth. In the context of our earlier observations on simple diatomic molecules, such as O_2 and NO, it became necessary to test the effect of larger molecules like nitrogen dioxide (NO_2), a paramagnetic gaseous molecule with one unpaired electron, on the paramagnetic properties of LiNc-BuO crystals. The effect of molecular NO_2 on the EPR linewidth and/or intensity of LiNc-BuO can trigger the application of the material for the detection and measurement of NO_2. Three different experiments were performed using NO_2 with LiNc-BuO crystals: (i) LiNc-BuO crystals were initially exposed to room air (~21% O_2) and then exposed to 1% NO_2(+99% N_2); (ii) LiNc-BuO crystals were first exposed to 100% N_2 and then to 1% NO_2(+99% N_2); and (iii) LiNc-BuO crystals were first exposed to room air and then 100% NO_2. The changes in the peak-to-peak linewidth and EPR intensity were monitored.

The first set of experiments was performed to determine whether NO_2 can replace O_2 molecules pre-internalized in the channels of LiNc-BuO crystals. The effect of 1% NO_2 on the EPR linewidth of LiNc-BuO crystals in room air (~21% O_2) is shown in Fig. 2A. The crystals showed a linewidth of 1.450 ± 0.022 G in room air. On subsequent exposure to 1% NO_2, there was a reduction in the linewidth to 0.320 ± 0.012 G with a response time of less than a minute. The crystals were then re-exposed to room air resulting in the width returning to 1.450 G, the original value of the linewidth of room air-exposed crystals. On the subsequent exposure of 100% N_2, the linewidth decreased to 0.280 G,

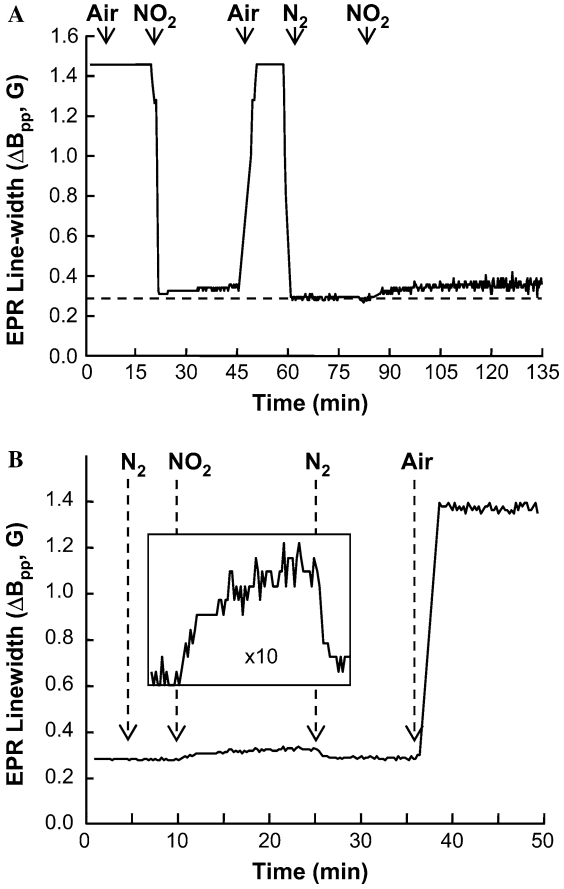

Fig. 2. Effect of 1% NO_2 gas on the EPR linewidth of LiNc-BuO microcrystals. The LiNc-BuO crystals were placed in gas-permeable Teflon tubing and the equilibrating gas was rapidly switched between room air (~21% O_2), 1% NO_2 (+99% N_2), and 100% N_2, as indicated. The plots show a representative of three independent experiments in each group (see text for mean ± SD). (A) Room air-exposed LiNc-BuO showed a linewidth of 1.450 G, which decreased to 0.325 G within 1 min of exposure. When the gas was switched to room air, the linewidth returned to 1.450 G. When exposed to pure N_2, the linewidth decreased to 0.280 G, and increased to 0.325 G on subsequent exposure to 1% NO_2. The sensitivity of linewidth of LiNc-BuO to NO_2 was calculated as 5.92 mG/mmHg. (B) LiNc-BuO crystals exposed to 100% nitrogen showed a linewidth of 0.280 G. When the crystals were exposed to 1% NO_2, the linewidth slowly increased (see the expanded view in the inset) to 0.325 G. When the gas was switched back to nitrogen, the linewidth decreased to 0.280 G, and when subsequently exposed to room air, the linewidth increased to 1.450 G.

which is the anoxic linewidth of LiNc-BuO. When the crystals were exposed again to 1% NO_2, an increase in linewidth to 0.320 G was observed. This process of linewidth modulation by NO_2 and O_2 was highly reversible. The sensitivity of LiNc-BuO to NO_2 was calculated from its anoxic linewidth and 1% NO_2-exposed linewidth as 5.26 ± 0.46 mG/mmHg, a value very similar to that of NO in LiNc-BuO [34]. The linewidth sensitivity to NO_2 was further verified using different compositions of NO_2 gas (0–1%) obtained by diluting the 1% gas with nitrogen. The data showed a linear response of linewidth to partial pressure of NO_2 in this range.

Additional experiments were performed to determine the effect of NO_2 in the absence of pre-internalized O_2 molecules in the channels of LiNc-BuO crystals. First, oxygen was replaced with 100% nitrogen and then the crystals were exposed to 1% NO_2. The effect of 1% NO_2 on the EPR linewidth of LiNc-BuO crystals kept under nitrogen is shown in Fig. 2B. LiNc-BuO microcrystals in a 100% N_2 atmosphere showed an anoxic linewidth of 0.280 ± 0.005 G. Exposure to 1% NO_2 gas, thereafter, resulted in an increase of linewidth to 0.320 ± 0.010 G. The response to NO_2, however, was gradual as can be seen from the inset of Fig. 2B. Upon switching back to 100% N_2, the linewidth reverted back to 0.280 G, suggesting that NO_2 molecules can freely diffuse in and out of the channels in the absence of oxygen. At this stage, exposure of the crystals to room air resulted in the linewidth increasing to 1.450 ± 0.015 G, the same as the initial room air linewidth of LiNc-BuO (cf. Fig. 2A). These gas-switching experiments clearly demonstrated the free transportability and mobility of NO_2 within the channels of this lattice.

These gas-exchanging experiments revealed that (i) a large molecule like NO_2 penetrated into the channel present in the LiNc-BuO crystal lattice; (ii) NO_2 easily replaced the smaller-sized oxygen present inside this lattice; (iii) the spins of NO_2 initially interacted with the spins of LiNc-BuO in a dipolar fashion due to its mobility in the channel, which was reflected by an increase of linewidth to 0.320 G, and this value was above the anoxic width of 0.280 G for the pure lattice; and (iv) the reactive NO_2 gas, upon its collision with the molecules of LiNc-BuO in the lattice, captured the unpaired electron of the latter, possibly to form a diamagnetic nitrite ion (vide infra), resulting in an irreversibly reduced EPR intensity due to the partial-to-total loss of paramagnetism of the LiNc-BuO crystals.

The EPR spectral intensity data of LiNc-BuO exposed to room air (~21% O_2) followed by exposure to 1% NO_2 is shown for representative experiment in Fig. 3 (solid line). The EPR intensity showed an initial increase, followed by a gradual decrease resulting in a complete reduction after about 90 min of continuous exposure to 1% NO_2. Since NO_2 is a highly reactive gas, it has possibly reacted with the LiNc-BuO crystal irreversibly, and this resulted in the loss of its EPR activity to a substantial extent. This was further confirmed by re-exposing the converted material to nitrogen gas and measuring the EPR intensity.

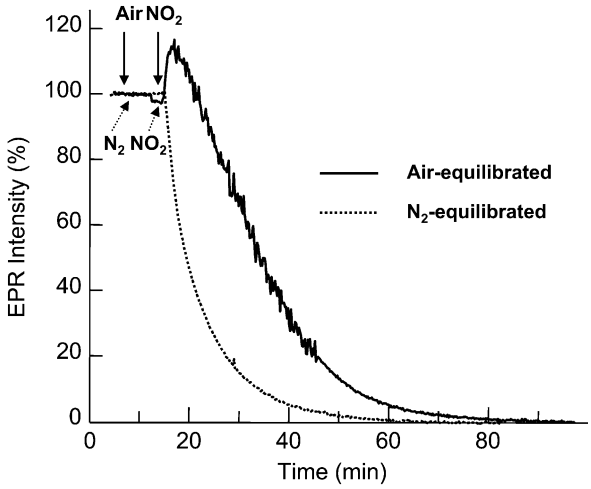

Fig. 3. Effect of 1% NO_2 gas on the EPR signal intensity of LiNc-BuO microcrystals. LiNc-BuO crystals, either pre-equilibrated with room air (solid line) or 100% N_2 (dashed line), were exposed to 1% NO_2 as indicated. The change in EPR intensity, measured by double-integration, of a representative experiment is shown. There is a gradual reduction in the EPR signal intensity leading to a complete reduction in 60–90 min of continuous exposure to NO_2 gas. A single exponential decay fit to the representative data shown in the plot revealed the decay half-time to be 11.4 min for the air- and 4.8 min for the nitrogen-equilibrated crystals.

The EPR intensity after re-exposure to N_2 gas did not show any increase at all. This clearly established that the LiNc-BuO molecule slowly lost its EPR activity on exposure to NO_2 gas for long periods of time. A single exponential decay fit to the experimental data from three separate experiments showed the decay half-time to be 10.2 ± 2.1 min (mean $\pm$ SD). It should be noted that the increase in EPR intensity of LiNc-BuO crystals immediately up on exposure to 1% NO_2 (Fig. 3, solid line) was not an artifact. This feature was reproducible on repeated cycles of gas exchange in a single experiment, as well as in independent measurements. We also observed similar increases when room air-exposed crystals were exposed to 0.5% NO_2 (+99.5% N_2) or 100% N_2 (data not shown). The relative increases in the intensity of LiNc-BuO exposed to 1% NO_2, 0.5% NO_2, and 100% N_2 were 13.2, 16.5, and 19.3%, respectively. The results seem to suggest that the increase is attributed to the removal of oxygen by nitrogen gas. We also observed a similar phenomenon occurring in LiPc crystals [32]. Unlike in solution, where the EPR intensity is unaffected by oxygen, in the solid state where the host spins are strongly exchange-coupled, the introduction or removal of oxygen is generally observed to cause changes in the paramagnetic susceptibility and EPR intensity. However, the exact nature of the mechanism of the increase observed on deoxygenation of LiNc-BuO is not clearly understood.

The effect of 1% NO_2 on the EPR spectral intensity data of LiNc-BuO, pre-exposed to 100% N_2, is shown for a representative experiment in Fig. 3 (dashed line). The EPR intensity gradually decreased as the LiNc-BuO crystals were continuously exposed to 1% NO_2. A complete loss

of signal intensity was observed after about 60 min of continuous exposure to 1% NO_2. A single exponential decay fit to the experimental data from three separate experiments showed the decay half-time to be 5.2 ± 0.9 min. The observed difference between the half-times of deoxygenation and oxygenation steps is attributed to the difference in the permeability of oxygen and nitrogen into the lattice. A recent report by Budd et al. [37] shows that phthalocyanine-based polymers have higher permeability coefficient for oxygen than nitrogen. Although we do not know the permeability coefficients of O_2, N_2, and NO_2 in LiNc-BuO lattice, we think that the difference may be due to the difficulty in replacing the oxygen present in the room air-exposed lattice by nitrogen or nitrogen dioxide. This is also confirmed by our observation of substantial differences in the rates of oxygenation versus deoxygenation processes in LiNc-BuO crystals [34].

It should be noted that although the EPR signal intensity of LiNc-BuO is dependent on the time of exposure to NO_2 gas, the measured linewidth is independent of the exposure time. Hence, the linewidth can be measured as long as the signal intensity (S/N) is adequate for linewidth determination. The data shown in Fig. 2 indicate that the linewidth can be measured for more than 30 min following exposure to 1% NO_2. Hence, in principle, it is possible to determine the concentration of NO_2 in any system by measuring the EPR linewidth of the LiNc-BuO crystals exposed to low concentrations of NO_2. A notable drawback is that the linewidth-based determination of NO_2 cannot be used in the presence of other paramagnetic gases such as O_2 and NO. However, it is possible to estimate the amount of NO_2 exposure from the decay kinetics of loss of signal intensity including time of exposure and rate constant. A more detailed investigation on the possible use of the signal loss data for accurate determination of very low levels of NO_2 is in progress.

The reduction in the EPR intensity of LiNc-BuO upon exposure to 1% NO_2 suggests the transformation of the crystals into an EPR inactive form, i.e., a diamagnetic species. This was further tested by increasing the concentration of NO_2. Exposure of the crystals to 100% NO_2 transiently broadened the EPR spectrum of LiNc-BuO as shown in Fig. 4. The broadened EPR spectrum completely disappeared after one minute of exposure. The increased linewidth observed upon exposure to 100% NO_2, suggests that, NO_2 is transported freely into the channels of LiNc-BuO crystals where spins are available for interaction with NO_2. This leads to the initially observed dipolar broadening at 35 s, in conformity with the earlier observations. The disappearance of the EPR spectrum after one minute of exposure to NO_2 gas indicates that the highly reactive NO_2 must have changed the spin property of LiNc-BuO. Also, when the NO_2-exposed LiNc-BuO crystals were further exposed to room air or nitrogen gas, no recovery of the EPR intensity was observed. The results, (i) the total disappearance of EPR signal within one minute of exposure to 100% NO_2 and (ii) the non-recovery of EPR signal

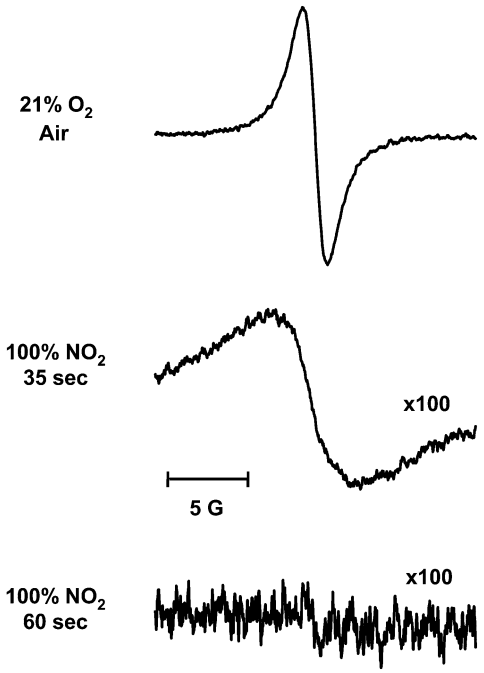

Fig. 4. Effect of 100% NO_2 gas on the EPR spectrum of LiNc-BuO crystals measured at room temperature. The spectra were acquired after exposure to 100% NO_2 at times as indicated. Following an initial broadening, the spectrum completely disappeared after one minute of exposure to NO_2.

intensity in the above experiment, reveal that LiNc-BuO crystals permit the NO_2 molecules to enter into the crystal channels in a manner similar to O_2 and NO [34], and the incorporated NO_2 molecules later react with the LiNc-BuO molecules resulting in the permanent loss of paramagnetism. The increase in EPR line-broadening and nearly zero EPR intensity after a very short time of exposure to 100% NO_2 gas (Fig. 4), in comparison with the similar effect of 1% NO_2 gas but over a period of nearly 60–90 min (Figs. 2 and 3), indicates that the line-broadening and intensity changes depend on the concentration of NO_2 at any given time. It can, therefore, be easily inferred that the number of effective collisions between gaseous NO_2 and LiNc-BuO decides the rate of conversion of paramagnetic LiNc-BuO to a diamagnetic species.

To understand how the interaction between NO_2 and LiNc-BuO leads to possible diamagnetic product(s) it is important to know the crystalline packing in LiNc-BuO. We have recently reported the X-ray crystal structure of LiNc-BuO as determined from powder X-ray diffraction analysis ([34]). A brief description of the packing arrangement is as follows. The analysis revealed that triclinic unit cells were arranged to form infinite channels along the *c*- and *a*-axes. The cross-sectional dimensions of the channels are not smaller than 10×6 Å^2, 6×4 Å^2, or 5×5 Å^2, along the *c*, *b*, or *a* axes, respectively. The presence of large and interconnected voids in the crystal structure could allow facile diffusion of large molecules, such as NO_2. Along the *a*-axis, an interplanar distance of 8.0 Å and a Li–Li distance of 14.9 Å separated the closest LiNc-BuO

molecules from the two neighboring dimers. On the other hand, in the *c*-direction, the planar spacing between the dimers was almost identical to the intra-dimer spacing of ~4.2 Å, and the adjacent dimers were glided from each other to have a Li–Li distance of 9.3 Å. This structural motif was crucial for allowing not only the small-size gases like O_2 (approximate size 2.8×3.9 Å^2), NO, and N_2 (approximate size 3.0×4.1 Å^2), but also larger-size gas NO_2 (approximate size 5.24×3.55 Å^2) to enter freely into the LiNc-BuO channel. The effect of NO_2 on the EPR linewidth of LiNc-BuO is seen in Figs. 2 and 4. The initial EPR line-broadening was due to the Heisenberg spin exchange between paramagnetic NO_2 and the two-dimensional spin diffusion along the stack axis of LiNc-BuO crystals which resulted in shortening of the spin–spin relaxation time of LiNc-BuO spins. Or, it is simply the dipolar effect of NO_2 on the exchange-narrowed EPR lines of the radicals. The effect was observable in the form of an increase in the linewidth of its EPR spectrum (Fig. 2B). However, when the concentration of NO_2 was increased to 100%, it led to the possibility of increased collisions between the radical electrons and NO_2 molecules, leading to electron-transfer resulting in the creation of diamagnetic species (vide infra).

While the effect of magnetic interaction between LiNc-BuO and NO_2 on the EPR linewidth is obvious, the nature of chemical interaction between them, leading to the loss of the LiNc-BuO paramagnetism, requires further investigation. Two possible interactions are considered: physisorption of NO_2 in the proximity of LiNc-BuO spins in the lattice; and oxidation of LiNc-BuO by NO_2. The former interaction may lead to a highly exchange-coupled radical pair resulting in the loss of observed EPR signal. The later interaction will result in the formation of LiNc-BuO$^+$ (diamagnetic) and nitrite (NO_2^-) ions. To obtain evidence for the presence of trapped NO_2 molecules and/or nitrite ion, we performed infra-red (IR) spectroscopic measurements on the transformed samples. The FT-IR spectra of LiNc-BuO lattice before and after exposure to 1% NO_2 gas for 1 h are shown in Fig. 5. As can be clearly seen in this figure, while the transmission spectrum in the region of 1800–800 cm^{-1} in the lattice prior to exposure to the gas is free of any broadening effect with many peaks corresponding to the organic modes, the same spectral region becomes not only broad but has new peaks either formed afresh or overlapping with the earlier modes after the oxidation of the LiNc-BuO ring system by NO_2. Three observations are unique: (i) a similar broadening of the absorption has been observed in thin films of nickel phthalocyanine exposed to NO_2 ([38]). (ii) The IR spectrum of LiNc-BuO exposed to NO_2 showed a band at 1721 cm^{-1} characteristic of free NO_2 trapped in the lattice. The band, however, was persistent in the transformed sample kept under vacuum at room temperature for 36 h (data not shown) indicating that part of the NO_2 could not be removed from the lattice because of its possibly getting trapped in some locations possibly due to some form of π–π interaction between the

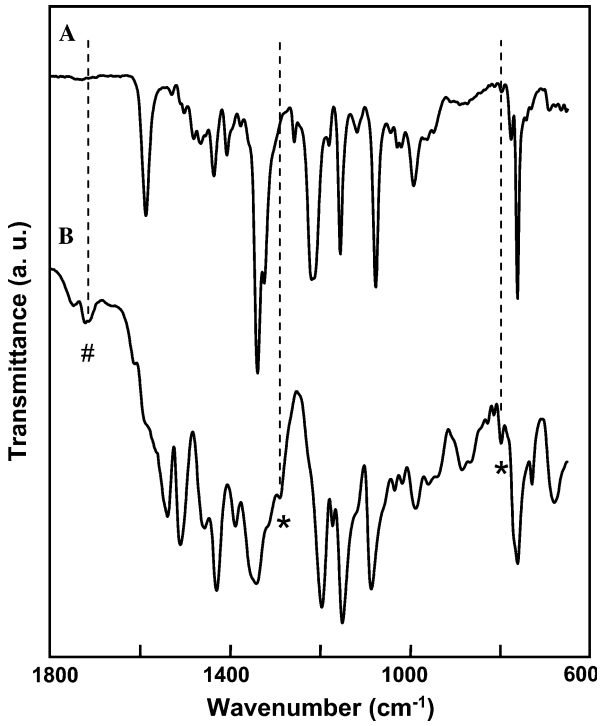

Fig. 5. FT-IR spectra of LiNc-BuO crystals before and after exposure to 1% NO_2 gas. (A) FT-IR spectrum of unexposed LiNc-BuO crystals. (B) FT-IR spectrum of LiNc-BuO crystals exposed to 1% NO_2 for 1 h. The broad absorption seen in (B) over the range 1800–800 cm^{-1} is attributed to oxidation of the LiNc-BuO ring system by NO_2. The band at 1721 cm^{-1} in (B) (marked by #) is due to free NO_2 trapped in the lattice. The bands at 1328 cm^{-1} and 828 cm^{-1} in (B) (marked by *) are indicative of nitrite ions.

gas and the ring system. (iii) One should also note that the nitrite ion when formed will have bands at $\nu_1 = 1328$ cm^{-1}, $\nu_2 = 828$ cm^{-1}, and $\nu_3 = 1261$ cm^{-1} ([39]), the first two being due to the stretching modes of N═O, N—O and the last one due to δ(O—N—O). The formation of the band at 828 cm^{-1} is obvious by its appearance though with low intensity. On the other hand, the anticipated band at 1328 cm^{-1}is very close to the already existing band in the pure LiNc-BuO lattice at ~1340 cm^{-1} and hence they have merged and broadened on exposure to the gas. Similarly, the band $\nu_3 = 1261$ cm^{-1} due to the nitrite ion formed by the oxidation of the lattice clearly merged into another band of the pure LiNc-BuO at 1210 cm^{-1} creating the large intensity overlapping band. The three bands system indicative of nitrite ion were observed in the treated sample. Initial physisorption of NO_2 in the vicinity of LiNc-BuO in the bulk lattice can lead to oxidation of LiNc-BuO to form LiNc-BuO$^+$ and NO_2^-. This is similar to the NO_2^--mediated oxidation of ruthenium phthalocyanine and naphthalocyanine thin films [40] and other phthalocyanines [41,42]. The IR spectrum of the 1% NO_2 exposed LiNc-BuO further indicates no damage to the lattice expect for the process of oxidation of the latter. The EPR and IR data put together clearly suggest that the predominant reaction is the oxidation of LiNc-BuO by NO_2 to give rise to diamagnetic LiNc-BuO$^+$ and nitrite ions.

4. Conclusions

The effect of NO_2 on LiNc-BuO crystals as measured by EPR spectroscopy indicated that the open channels present in LiNc-BuO were large enough to permit the easy diffusion of larger paramagnetic gas such as NO_2. The spectral width was sensitive to the presence of NO_2 gas with its unpaired electron providing a dipolar effect on the unpaired electron spins in LiNc-BuO. The line-broadening effect was similar to that of molecular O_2 and NO in LiNc-BuO crystals. However, at higher concentrations of NO_2 (100%), increased collisions between the gas and lattice lead to a diamagnetic lattice, apparently due to the one-electron oxidation of LiNc-BuO by gaseous NO_2. The observed results are consistent with the EPR and IR spectroscopic data. These results suggest that LiNc-BuO may be used as a very sensitive NO_2 sensor which works at room temperature and may open a new opportunity for the application of LiNc-BuO as a chemical sensor for NO_2, especially in trace amounts.

Acknowledgment

This study was supported by NIH Grant EB 004031.

References

[1] L.X. Cao, L.H. Huo, G.C. Ping, D.M. Wang, G.F. Zeng, S.Q. Xi, Particulate multilayers prepared from surfactant-stabilized SnO_2 nanoparticles, Thin Solid Films 347 (1999) 258–262.
[2] N.I. Kovtyukhova, P.J. Ouivie, B.R. Martin, T.E. Mallouk, S.A. Chizhik, E.V. Buzaneva, A.D. Gorchinskiy, Layer-by-layer assembly of ultrathin composite films from micron-sized graphite oxide sheets and polycations, Chem. Mater. 11 (1999) 771–778.
[3] L.S. Li, Z. Hui, Y. Chen, X.T. Zhang, X. Peng, Z. Liu, T.J. Li, Preparation and organized assembly of nanoparticulate TiO_2–stearate alternating Langmuir-blodgett films, J. Colloid Interface Sci. 192 (1997) 275–280.
[4] H.X. Zeng, Iron oxides gas sensitive materials and their use, J. Instrument Mater. (Chinese) B 20 (1988) 228–234.
[5] K. Hara, N. Nishida, H_2 sensors using Fe_2O_3-based thin film, Sens. Actuators B 20 (1994) 181–186.
[6] A.S. Poghossian, H.V. Abovian, V.M. Aroutiounian, Selective petrol vapour sensor based on an Fe_2O_3 thin film, Sens. Actuators B 18/19 (1994) 155–157.
[7] J. Peng, C.C. Chai, A study of the sensing characteristics of Fe_2O_3 gas-sensing thin film, Sens. Actuators B 13/14 (1993) 591–593.
[8] D.G. Zhu, D.F. Cui, M. Harris, M.C. Petty, Gas-sensing using Langmuir-blodgett-films of a ruthenium porphyrin, Sens. Actuators 12 (1993) 111–114.
[9] J.D. Wright, Gas adsorption on phthalocyanine and its effect on electrical properties, Prog. Surf. Sci. 31 (1989) 1–60.
[10] J.D. Wright, P. Roisin, G.P. Rigby, R.J.M. Nolte, M.J. Cook, S.C. Thorpe, Crowned and liquid-crystalline phthalocyanines as gas-sensor materials, Sens. Actuators 13–14 (1994) 276–280.
[11] P.S. Vukusic, J.R. Sambles, Cobalt phthalocyanine as a basis for the optical sensing of nitrogen-dioxide using surface-plasmon resonance, Thin Solid Films 221 (1992) 311–317.
[12] P.N. Barlett, S.K. Lingchung, Conducting polymers gas sensors. 3. Results for 4 different polymers and 5 different vapors, Sens. Actuators 20 (1989) 287–292.
[13] T. Hanawa, H. Yoneyama, Gas sensitivities of polypyrrole films doped chemically in the gas phase, Synth. Met. 30 (1989) 341–350.
[14] T. Hanawa, S. Kuwabata, H. Hashimoto, H. Yoneyama, Gas sensitivities of electropolymerized polythiophenes films, Synth. Met. 30 (1989) 173–181.
[15] C.C. Lenzoff, A.B.P. Lever, Phthalocyanines: Properties and Applications, VCH, New York, 1996.
[16] N.B. McKeown, Phthalocyanine Materials: Synthesis, Structure and Function, Cambridge University Press, Cambridge, 1998.
[17] A.W. Snow, W.R. Barger, Phthalocyanines: Properties and Applications, VCH, Cambridge, UK, 1989.
[18] A. Generosi, V.R. Albertini, G. Rossi, G. Pennesi, R. Caminiti, Energy dispersive X-ray reflectometry of the NO_2 interaction with ruthenium phthalocyanine films, J. Phys. Chem. B 107 (2003) 575–579.
[19] J.C. Hsieh, C.J. Liu, Y.H. Ju, Response characteristics of lead phthalocyanine gas sensor: effects of film thickness and crystal morphology, Thin Solid Films 322 (1998) 98–103.
[20] Y. Sadaoka, T.A. Jones, W. Gopel, Effect of heat treatment on the electrical conductance of lead phthalocyanine films for NO_2 gas detection, J. Mater. Sci. Lett. 8 (1989) 1095–1097.
[21] Y. Sadaoka, T.A. Jones, G.S. Revell, W. Gopel, Effects of morphology on NO_2 detection in air at room temperature with phthalocyanine thin films, J. Mater. Sci. 25 (1990) 5257–5268.
[22] C.J. Liu, J.C. Hsieh, Y.H. Ju, Response characteristics of lead phthalocyanine gas sensor: effects of operating temperature and postdeposition annealing, J. Vac. Sci. Technol. A 14 (1996) 753–756.
[23] D. Campbell, R.A. Collins, A study of interaction between nitrogen dioxide and PbPc using electrical conduction and optical absorption, Thin Solid Films 295 (1997) 277–282.
[24] T. Kouzeki, S. Tatezono, H. Yanagi, Electrochromism of orientation controlled naphthalocyanine thin film, J. Phys. Chem. 100 (1996) 20097–20102.
[25] H. Yanagi, Y. Kanbayashi, D. Schlettwein, D. Woehrle, N.R. Armstrong, Photoelectrochemical investigations on naphthalocyanine derivatives in thin films, J. Phys. Chem. 98 (1994) 4760–4766.
[26] M. Shopova, D. Woehrle, V. Mantareva, S. Mueller, Naphthalocyanine-complexes as potential photosensitizers for PDT of tumors, J. Biomed. Opt. 4 (1999) 276–285.
[27] M.E. El-Khouly, L.M. Rogers, M.E. Zandler, G. Suresh, M. Fujitsuka, O. Ito, F. D'Souza, Studies on intra-supramolecular and intermolecular electron-transfer processes between zinc naphthalocyanine and imidazole-appended fullerene, Chem. Phys. Chem. 4 (2003) 474–481.
[28] K.P. Unnikrishnan, J. Thomas, V.P.N. Nampoori, C.P.G. Vallabhan, Third order nonlinear optical studies in europium naphthalocyanine using degenerate four wave mixing and Z-scan, Opt. Comm. 204 (2002) 385–390.
[29] R.A. Collins, K.A. Mohammed, Gas sensitivity of some metal phthalocyanines, J. Appl. Phys. 21 (1988) 154–161.
[30] G. Ilangovan, A. Manivannan, H. Li, H. Yanagi, J.L. Zweier, P. Kuppusamy, A naphthalocyanine-based EPR probe for localized measurements of tissue oxygenation, Free Radic. Biol. Med. 32 (2002) 139–147.
[31] A. Manivannan, H. Yanagi, G. Ilangovan, P. Kuppusamy, Lithium naphthalocyanine as a new molecular radical probe for electron paramagnetic resonance oximetry, J. Magn. Magn. Mater. 233 (2001) L131–L135.
[32] G. Ilangovan, J.L. Zweier, P. Kuppusamy, Mechanism of oxygen-induced EPR line broadening in lithium phthalocyanine microcrystals, J. Magn. Reson. 170 (2004) 42–48.
[33] R.P. Pandian, N.L. Parinandi, G. Ilangovan, J.L. Zweier, P. Kuppusamy, Novel particulate spin probe for targeted determination of oxygen in cells and tissues, Free Radic. Biol. Med. 35 (2003) 1138–1148.
[34] R.P. Pandian, K. Young-Il, P.M. Woodward, J.L. Zweier, P.T. Manoharan, P. Kuppusamy, The open molecular framework in lithium octa-*n*-butoxy-naphthalocyanine paramagnetic crystal: implications for the detection of oxygen and nitric oxide by EPR spectroscopy, J. Mater. Chem. (2006) (accepted).

[35] V.M. Petrusevski, M. Taseska, M. Monkovic, Reaction of copper with fuming nitric acid: a novel lecture experiment in passivation, Chemical Educator 10 (2005) 208–210.
[36] D. Kolbasov, J.R. Norris, Contribution of colliding parallel electron spins to electron paramagnetic resonance spectral narrowing, J. Chem. Phys. 118 (2003) 5582–5586.
[37] P.B. Budd, N.B. Mckeown, D. Fritsch, Free volume and intrinsic microporosity in polymers, J. Mater. Chem. 15 (2005) 1977–1986.
[38] K.F. Schoch, T.A. Temofonte, IR response of phthalocyanine thin films to nitrogen dioxide, Thin Solid Films 165 (1988) 83–89.
[39] K. Nakamoto, Infrared Spectra of Inorganic and Coordination Compounds, Wiley Interscience, New York, 1963.
[40] M. Passard, A. Pauly, J.P. Germain, C. Maleysson, Influence of NO_2 on the electrical conductivity of luteium phthalo-naphthalocyanine thin films, Synth. Met. 80 (1996) 25–28.
[41] S. Chakane, A. Gokarna, S.V. Bhoraskar, Metallophthalocyanine coated porous silicon gas sensor selective to NO_2, Sens. Actuators B 92 (2003) 1–5.
[42] G.L. Pakhomov, V.N. Spector, M.C. Anglada, J.M. Ribo, C. Muller, Some trends in sorption processes on thin film phthalocyanine films, Mendeleev Commun. (1996) 163–165.